Conducting Systems Based on Styrene–Butadiene-*Block*–Copolymers: Microstructural Characterization

J. L. ACOSTA, L. GONZÁLEZ, C. DEL RÍO, C. OJEDA A. RODRÍGUEZ

Instituto de Ciencia y Tecnología de Polímeros del CSIC, C/ Juan de la Cierva 3, 28006 Madrid, España

Received 7 September 2000; accepted 14 August 2001

ABSTRACT: This work reports on the preparation and structural and electrical characterization of composites consisting of HSBR, polypropylene (PP), and carbon black (CB) blends, comparing the data obtained from more or less rich PP samples. Structural analysis provided evidence of the plasticizing or crosslinked effects on the properties of composites, when CB is present in the initial system, as well as of the excellent conducting properties of CB composites. © 2002 John Wiley & Sons, Inc. J Appl Polym Sci 84: 646–653, 2002; DOI 10.1002/app.10360

Key words: conducting polymers; composites; DSC; membranes

INTRODUCTION

Fuel cells[1–4] are systems capable of continuously generating electricity from a fuel, their performance being considerably better than the combustion systems presently in use. Fuel cells are expected to play, both in the short and in the long term, an important part in sustainable energy supply, as they allow for considerable energy savings, as well as for diversifying energy sources. In addition, and due to their excellent performance, CO_2 emission by fuel cells is much lower than that of internal combustion engines per energy unit generated, apart from absolute avoidance of other pollutants (NO_x, SO_2, hydrocarbons, etc.). All these benefits and properties qualify fuel cells as ideal candidates for *automotive* applications, one of the most formidable pollutant and greenhouse gas emission sources of our time. The most adequate cells for these applications are the so-called proton-exchange-membrane fuel cells (PEMFCs), which operate close to room temperature and whose essential elements are a proton-conducting polymer film and an electrocatalyst with supports on both sides.

One of the most important components of fuel cells are the bipolar plates,[5–9] to date manufactured of graphite. Conducting composites have been suggested to replace this raw material. Considering the state of the art, the successful obtention of these systems (polymer composites with conducting additives) depends on the adequate choice of the polymer system. Contrary to what was thought some years ago, the polymer matrix is not only the support of the filler but also plays an important role in composite performance: (a) it favors particle interconnectivity (percolation); (b) it favors electrical conductivity through a tunnel-type mechanism in case conductivity is not very good; and (c) it has to be capable of taking up large amounts of additive without deteriorating its mechanical properties, which are accountable for both the transfer mechanisms and the dimensional stability of the resulting material.

There exist several materials as candidates for bipolar plates in fuel cells. In this research we developed and characterized composites based on

Correspondence to: J. L. Acosta (acosta@ictp.csic.es).
Contract grant sponsor: Regional Government of Madrid.

Table I Dynamo-Mechanical Analysis (DMA) of the Samples

Samples	Composition H-SBR/PP (wt %)	Composition NC	$T_{g(PBH)}$ (°C)	$T_{g(PP)}$ (°C)	$T_{g(PS)}$ (°C)
CP-10	50/50	0	−42.3	15.1	105.7
CP-11	50/50	10	−42.5	10.3	105.1
CP-12	50/50	20	−42.2	10.8	108.3
CP-13	50/50	30	−42.2	10.9	110.6
CP-14	50/50	40	−42.4	10.4	114.1
CP-15	50/50	50	−40.2	10.5	116.4
CP-20	70/30	0	−39.6	11.2	104.5
CP-21	70/30	10	−42.2	8.4	106.7
CP-22	70/30	20	−42.4	—	109.7
CP-23	70/30	30	−42.9	—	112.0
CP-24	70/30	40	−42.6	—	115.5
CP-25	70/30	50	−42.3	—	112.2

hydrogenated styrene–butadiene block copolymers.

EXPERIMENTAL

The elastomeric thermoplast (HSBR) was an ethylene–butylene/styrene (70/30) copolymer obtained by means of SBR hydrogenation. It possesses a linear structure and an insaturation level below 1% and was supplied by Repsol-YPF Química under the trade name CALPRENE H6120. The isotactic polypropylene (PP) used was of the ISPLEN PP-050 type as supplied by Repsol Químicas, with a yield index of 6.0 g/10 min. The carbon black used was the Cabot product Black Pearls 2000.

Blends were prepared in a Rheomix 600-Haake with Banbury type rotors at 180°C blending temperature until constant torque par (homogeneous dispersion), feeding the HSBR and PP simultaneously into the blending chamber; the chamber was purged with Nitrogen. Carbon black was incorporated once the PP had molten. The blending time was 6 and 12 min.

Sheets of 10 × 10 cm were molded in a Collins press at 200 kg/cm^2 and 180°C temperature.

Mechanical experiments were performed under standard conditions using an Instron mod. 430, at room temperature (25°C); the strain rate was 10 mm s^{-1}. The tensile modulus E was determined by the usual procedure from the slope of the initial part of the stress–strain curve. Five specimens were studied in each case.

The dynamic mechanical measurements were conducted in a dynamic mechanical thermal analyzer TA Instruments 983 at 1 Hz, in the temperature range of 173–413 K and at a rate of 2 K min^{-1}.

The DSC thermograms were then recorded at a heating rate of 5°C/min. Isothermal crystallization and melting behavior were followed using a Mettler 4000 differential scanning calorimeter. The samples were brought to melt at 473 K for 10 min and then cooled (350 K/min) to the desired crystallization temperature. Melting temperatures were obtained by heating the crystallized samples at a rate of 10 K/min.

DC conductivity measurements were carried out using a Hewlett-Packard Model HP-6614C coupled to a computer, at 1 and 0.1 V and over a temperature range of 30 to 110°C.

RESULTS AND DISCUSSION

Glass Transition Temperature Analysis (T_g)

Glass transition temperatures were determined by means of dynamic mechanical analysis (DMA). Table I compiles the results obtained for all the experimental samples, each of them at five different CB portions.

The dynamic mechanical spectra are compiled in Figures 1 and 2, where the δ-value of each

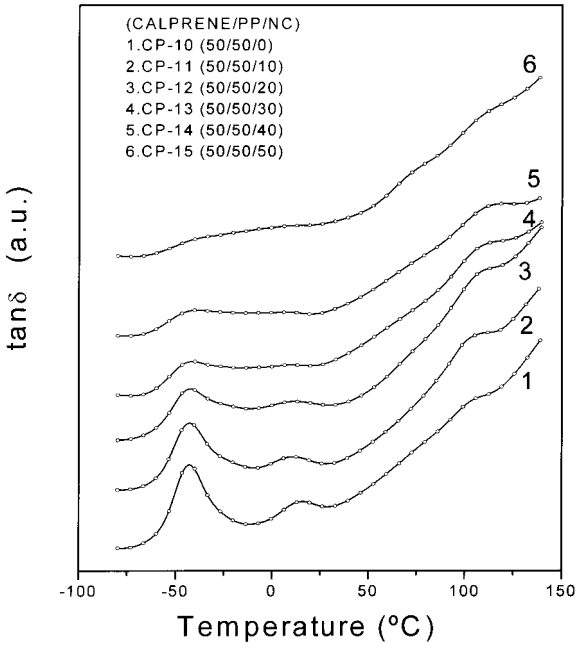

Figure 1 DMA analysis of the Calprene/PP/CB samples measured at 5 Hz.

individual sample is plotted against temperature. Figure 1 shows the spectra of the HSBR/PP (50/50) samples and five CB percentiles. For the CB-free sample, there appear three clearly defined glass transitions corresponding to each of the three components of the system: at −42.3°C for the polybutadiene units in HSBR; at 15.1°C for PP; and at 105.7°C for the styrene portion in HSBR (Fig. 1-1). With increasing CB content in the blends, there appear drastic changes in the microstructure of the respective composites, as proven by the remarkable shifts of the glass transition temperatures in all the samples: on the one hand, note that the transition related to the T_g of the hydrogenated polybutadiene sequences in HSBR is becoming fainter, yet rising proportionally at the same time, as a consequence of increasing CB content, which fact confirms the effect of greater stiffness conferred by CB onto the polybutadiene groups in HSBR, due to their adherence to the CB surface. The same effect can be observed for the glass transition of the polystyrene backbone in HSBR, thus legitimating the view that a phenomenon of a similar nature is involved here, as was identified for the polybutadiene backbone in the composite. The opposite phenomenon, however, is observed to occur in PP, when examining the respective changes undergone by its T_gs: inversely proportionate to increasing CB content the strain corresponding to the T_g of polypropylene decreases, which is indicative of the plasticizing effect exerted by CB on the PP backbone, this latter effect being proportionate to CB content in the blend.

Identical results were found, when interpreting the dynamic mechanical spectra of the samples based on 70/30 HSBR/PP composites (Fig. 2), thus serving as a confirmation of the findings mentioned above.

In the light of the microstructural changes recorded in terms of CB incorporation, it is possible to predict the thermal behavior of the material when cast into components.

Isothermal Crystallization Kinetic

Tables II and III compile the kinetic parameters of isothermal PP crystallization for the samples under study, data which were obtained from the Avrami equation. The data relating to the isothermal crystallization kinetics of the binary and ternary composites were analyzed on the basis of the Avrami equation,[10] which gives the variation in crystalline content over time at a constant crystallization temperature for a molten sample:

$$X(T) = 1 - \exp(-Kt^n)$$

where $X(T)$ is the weight fraction of crystallized material at time t, K represents the rate constant

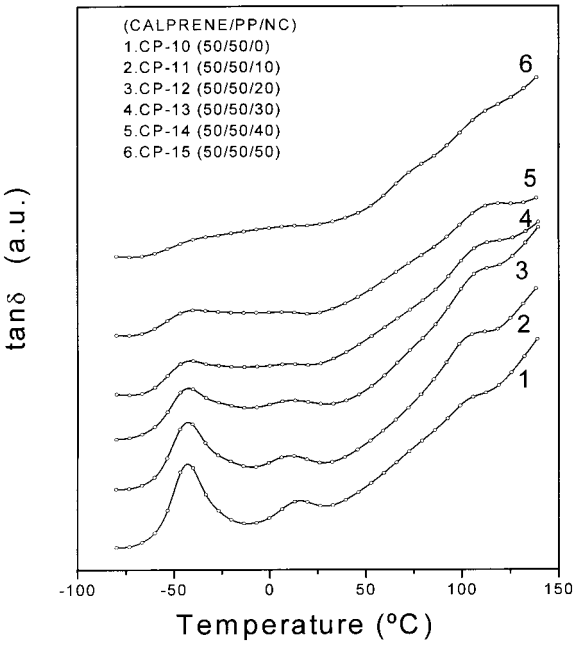

Figure 2 DMA analysis of the Calprene/PP/CB samples measured at 5 Hz.

Table II Kinetic Parameters of the Samples

Samples	Composition H-SBR/PP (wt %)	Composition NC	T_c K	T_m K	n	log K (min^{-n})
CP-10	50/50	0	401	439.0	2.22	−1.459
			402	439.5	2.15	−1.638
			403	439.5	2.30	−1.889
			404	440.0	2.41	−2.276
CP-11	50/50	10	401	438.5	2.01	−1.131
			402	438.5	2.06	−1.343
			403	438.9	2.13	−1.609
			404	439.4	2.16	−1.847
			405	439.8	2.17	−2.068
CP-12	50/50	20	399	438.0	1.98	−0.676
			400	438.1	2.01	−0.842
			401	438.4	2.05	−1.003
			402	438.5	2.12	−1.272
			403	438.7	2.15	−1.596
CP-13	50/50	30	399	438.1	1.99	−0.775
			400	438.1	2.05	−0.962
			401	438.1	2.04	−1.144
			402	439.6	2.16	−1.456
			403	439.8	2.18	−1.700
CP-14	50/50	40	399	437.1	2.21	−0.882
			400	437.1	2.41	−1.293
			401	437.1	2.36	−1.535
			402	437.1	2.14	−1.384
			403	437.3	2.26	−1.958
CP-15	50/50	50	399	435.5	2.10	−0.781
			400	435.5	1.94	−0.860
			401	435.5	1.89	−1.024
			402	435.0	1.94	−1.275
			403	435.7	1.87	−1.430

of the crystallization process, and n is the Avrami exponent, which depends on the type of nucleation taking place and the growth geometry. The n and K values were obtained from the slopes and intercepts, respectively, of plots of $\log\{-\ln[1 - X(T)]\}$ against $\log t$ for degrees of crystallinity below 30% and for each crystallization temperature.

Figure 3(A) shows the melting point variation of the PP portion contained in the samples as a function CB concentration for the two families: (1) HSBR/PP (50/50) and (2) HSBR/PP (70/30). In all cases the melting point is observed to drop slightly with increasing CB portion in the sample, this drop becoming much more prominent at CB concentrations above 30%, due to the braking effect exerted by the CB particles on PP crystallization. Hence, the PP spherulites formed at high CB content are considerably smaller than in the filler-free instances, so that their melting temperature is also respectively lower. The T_m drop is most prominent in the blends with the lowest PP portion (graph 2 in Fig. 3). Another approach to explaining the decrease in T_m as a function of increasing CB content in the blend is by means of the plasticizing effect exerted by CB on the microstructure of the composite, as inferred from T_g analysis, commented on above.

Figure 3(B) illustrates the effect exerted by CB on Avrami's exponent n, i.e., on the growth geometry of the PP spherulites in the polymeric matrix, comparing the 30% to the 50% PP family. In both families the effect proves to be similar: the value of n remains constant over a considerably broad CB range and diminishes only for the higher CB concentrations. For the HSBR/PP (70/

Table III Kinetic Parameters of the Samples

Samples	Composition H-SBR/PP (wt %)	Composition NC	T_c K	T_m K	n	log K (min^{-n})
CP-20	70/30	0	397	437.5	1.83	−0.729
			398	438.0	2.05	−1.048
			399	438.0	2.03	−1.242
			400	438.5	2.20	−1.619
			401	438.7	2.22	−1.879
CP-21	70/30	10	397	437.5	1.76	−0.009
			398	437.5	1.90	−0.270
			399	438.0	2.13	−0.565
			400	437.9	2.49	−1.163
			401	438.3	2.36	−1.326
CP-22	70/30	20	397	437.6	2.06	−0.401
			398	437.6	2.22	−0.716
			399	437.6	2.36	−0.996
			400	438.1	2.38	−1.317
			401	438.1	2.36	−1.502
CP-23	70/30	30	397	437.6	2.29	−0.619
			398	437.6	2.18	−0.846
			399	438.1	2.28	−1.084
			400	438.1	2.25	−1.283
			401	438.3	2.22	−1.432
CP-24	70/30	40	397	436.3	2.53	−1.118
			398	436.7	2.49	−1.124
			399	436.7	2.57	−1.665
			400	436.7	2.18	−1.649
			401	436.9	2.26	−1.930
CP-25	70/30	50	397	433.6	1.35	−0.067
			398	434.1	1.43	−0.255
			399	434.0	1.54	−0.418
			400	434.0	1.58	−0.557
			401	433.4	1.69	−0.801

30) family the value of n moves around $n = 2$. When increasing the PP portion in the blend, i.e., HSBR/PP (50/50), the value of n increases to $n = 2.5$. In the former case, spherulite growth may be considered bidimensional over the whole range of CB concentrations. The same is true for the

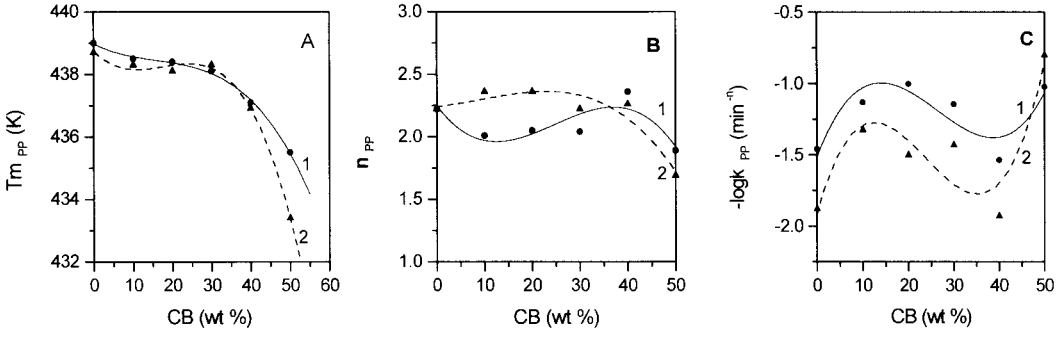

Figure 3 Analysis of Avrami kinetic parameters as a function of CB concentration (T_c = 401 K). 1: HSBR/PP(50/50) and 2: HSBR/PP(70/30).

50/50 family, however, implying some tridimensional growth, as a consequence of the changes in PP spherulite nucleation produced by the surface activity of CB.

The last kinetic parameter to be assessed was the crystallization rate constant of the PP component in the different composites. As can be seen in Figure 3(C), there exists behavioral parallelism, when comparing the 30% PP family to the 50% one. But there also exist appreciable differences, which come to light when comparing the effect of CB concentration within one and the same sample family. In both cases and up to a CB percentage of 10% the PP crystallization rate increases considerably, compared to the respective filler-free sample. For any CB content between 10% and around 40% the rate is observed to diminish slightly to show a drastic increase for the 50% CB sample. The explanation of these three clearly defined trenches in the behavior of the PP crystallization rate in the presence of CB has to be sought in the existence of two effects occurring simultaneously in the material: on the one hand, the barrier set up by the CB particles slowing down PP spherulite growth, and, on the other hand, the specific interactions taking place between each of the polymer components and the activity proper of the filler surface. The final balance of both these actions results in the behavior described.

As can be seen in Figure 3(C), both families show a similar behavior. The only difference relates to the rate value. For the higher PP concentration the crystallization rate logically is faster than for the 70/30 family.

Mechanical Properties

The stress–strain curves of the composites are shown in Figure 4. With the presence of a semic-

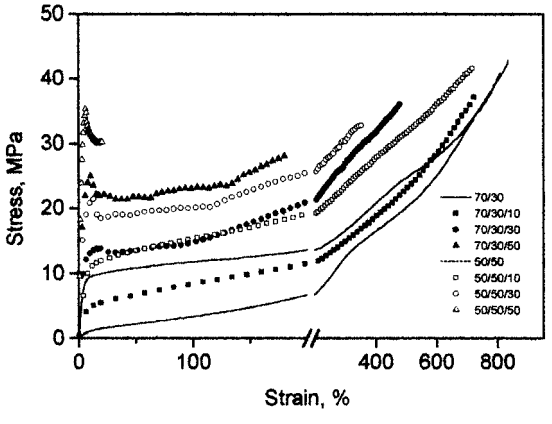

Figure 4 Stress–strain curves of the samples.

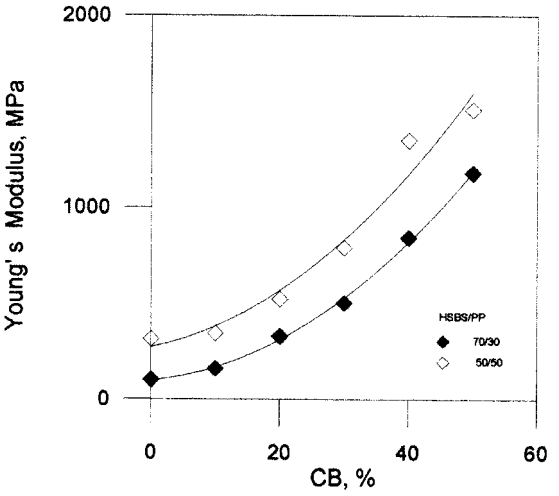

Figure 5 Young's modulus vs. CB contain.

rystalline polymer (PP) in the composite the yielding mechanism is produced. The unfilled low PP content sample presents a strain comparable to the unfilled elastomer. The composite with the greater PP portion, however, already shows a yielding behavior, even in the absence of the filler. The initial modulus proves to increase significantly with the addition of carbon black.

In general, the samples containing filler below the percolation threshold deform uniformly to fracture, at a stress and strain that are comparable to the fracture characteristics of the unfilled polymer blend. Above the percolation threshold yielding with formation of a well-defined neck is observed. This tendency to yield may be related to filler debonding from the matrix and the formation of cavities, which act like flaws.

Local stress concentration increases local strain, thus causing necking instability. In the 50/50 (w/w) family, when the composition exceeds the percolation threshold, the fracture strain decreases dramatically. Excepting this composite, all other samples deform uniformly to a strain similar to or lower than that of the unfilled series.

The effects of the filler on the Young modulus are shown in Figure 5, where a variation is observed as a function of PP content. Tensile strength decreases inversely proportionate to carbon black concentration, as shown in Figure 6. This decrease is greater in the composites with the greater PP portion.

Electrical Properties

One of the most relevant properties that these materials must possess when they are to be em-

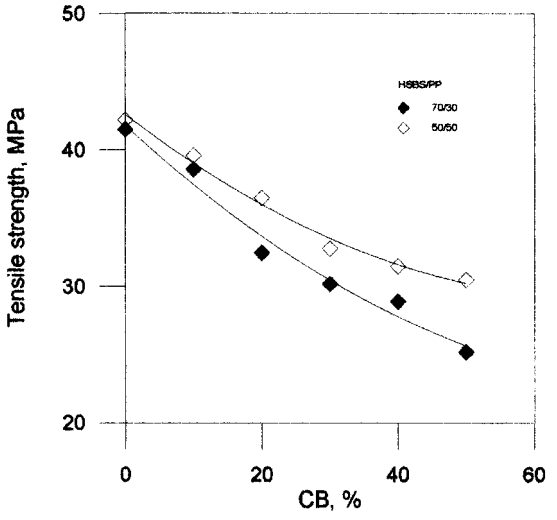

Figure 6 Tensile strength vs. CB contain.

ployed as bipolar plates in polymeric membrane fuel cells refers to high electron conductivity. To the purpose of determining the electrical properties of the experimental composites, they were subjected to a complex impedance spectroscopy study, as well as to the four-point method. The conductivity values obtained are compiled in Tables IV and V, the respective graphs being shown in Figure 7, in which the two experimental composite families are compared. For both series conductivity increases spectacularly between 10 and 20% CB, as in this range the particle percolation peak is reached.

When comparing the conductivity values achieved by the 30 and 50% PP families, no essential differences are detected, i.e., independent of PP content, the composites show comparable conductivity values, except for low filler content (approximately 10% CB), where the 30% PP family achieves a notably lower conductivity, a difference which disappears when increasing CB content.

Tables IV and V show conductivity to decrease with increasing test temperature, which fact, again, confirms the electronic nature of the transfer.

Table IV Electrical Conductivity of the Samples

Samples	Composition H-SBR/PP (wt %)	Composition NC	Temp (°C)	Conductivity ($S \cdot cm^{-1}$)
CP-10	50/50	0	30	$8.78 \cdot 10^{-9}$
			50	$7.39 \cdot 10^{-9}$
			75	$6.56 \cdot 10^{-9}$
			100	$7.05 \cdot 10^{-9}$
CP-11	50/50	10	30	$3.04 \cdot 10^{-4}$
			50	$2.94 \cdot 10^{-4}$
			75	$2.12 \cdot 10^{-4}$
			100	$1.70 \cdot 10^{-4}$
CP-12	50/50	20	30	$1.67 \cdot 10^{-2}$
			50	$2.25 \cdot 10^{-2}$
			75	$1.97 \cdot 10^{-2}$
			100	$9.09 \cdot 10^{-3}$
CP-13	50/50	30	30	$5.60 \cdot 10^{-2}$
			50	$6.54 \cdot 10^{-2}$
			75	$6.82 \cdot 10^{-2}$
			100	$6.02 \cdot 10^{-2}$
CP-14	50/50	40	30	$8.83 \cdot 10^{-2}$
			50	$8.89 \cdot 10^{-2}$
			75	$8.45 \cdot 10^{-2}$
			100	$1.49 \cdot 10^{-2}$
CP-15	50/50	50	30	$1.22 \cdot 10^{-1}$
			50	$2.01 \cdot 10^{-1}$
			75	$1.76 \cdot 10^{-1}$
			100	$7.68 \cdot 10^{-2}$

Table V Electrical Conductivity of the Samples

Samples	Composition H-SBR/PP (wt %)	Composition NC	Temp (°C)	Conductivity ($S \cdot cm^{-1}$)
CP-20	70/30	0	30	$8.75 \cdot 10^{-9}$
			50	$6.95 \cdot 10^{-9}$
			75	$8.30 \cdot 10^{-9}$
			100	$7.69 \cdot 10^{-9}$
CP-21	70/30	10	30	$2.33 \cdot 10^{-7}$
			50	$2.18 \cdot 10^{-7}$
			75	$1.79 \cdot 10^{-7}$
			100	$1.63 \cdot 10^{-7}$
CP-22	70/30	20	30	$7.54 \cdot 10^{-3}$
			50	$6.61 \cdot 10^{-3}$
			75	$4.32 \cdot 10^{-3}$
			100	$3.12 \cdot 10^{-3}$
CP-23	70/30	30	30	$8.36 \cdot 10^{-2}$
			50	$9.71 \cdot 10^{-2}$
			75	$3.45 \cdot 10^{-2}$
			100	$1.84 \cdot 10^{-2}$
CP-24	70/30	40	30	$1.47 \cdot 10^{-1}$
			50	$1.40 \cdot 10^{-1}$
			75	$4.88 \cdot 10^{-2}$
			100	$1.31 \cdot 10^{-2}$
CP-25	70/30	50	30	$1.68 \cdot 10^{-1}$
			50	$1.58 \cdot 10^{-1}$
			75	$8.50 \cdot 10^{-2}$
			100	$2.52 \cdot 10^{-2}$

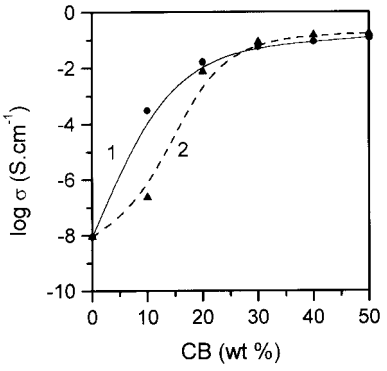

Figure 7 Conductivity as a function of CB concentration; (—) HSBR/PP (50/50) and (- - -) HSBR/PP (70/30).

CONCLUSION

In the light of the data obtained from this research it is legitimate to conclude that carbon black affects the microstructure and the electrical properties of EPDM/PP blends containing a CB filler in different proportions. On the one hand, CB acts as a plasticizer, and thus influences the chemical structure of PP, shifting both the glass transition temperature and the melting point towards lower temperature ranges. At the same time, CB acts as a crosslinking agent vis à vis the butadiene or styrene parts in HSBR, shifting the respective glass transitions towards higher temperature ranges. This phenomenon has a direct impact on the mechanical properties of the composite, in such a way that, in the presence of CB, the processing conditions improve, as well as the mechanical properties, compared to the behavior of CB-free systems.

By the same token, CB has a slight inhibiting effect on the PP spherulite growth geometry in the different composites. In contrast, CB, at high concentrations, is capable of inducing crystalline nucleus formation on its surface, which motivates an apparent increase in the crystal growth rate.

Finally, the conductivity values reached and the unproblematic processing of these composites qualify them as adequate base materials in bipolar plates.

We express our sincere thanks to the Regional Government of Madrid (Spain) for the funding of this project and the support provided in the implementation of this research.

REFERENCES

1. A Ten Year Fuel Cell Research, Development and Demonstration Strategy for Europe; European Commisions, DGXII and DGXVII.
2. Ralph, T. P. Platinum Metals Rev 1997, 41, 102.
3. Patil, P.; Zegers, P. J Power Sources 1994, 49, 169.
4. Adcock, P. L., et al. J Power Sources 1992, 37, 201.
5. Dyson, R. W. Speciality Polymers; Blackie, Chapman and Hall: New York, 1987.
6. Blythe, A. R. Electrical Properties of Polymers; Cambridge University Press: Cambridge, 1979.
7. Beck, F.; Suden, G. T.; Tormin, U.; Boinowitz, T. Electrochim Acta 1996, 41, 933.
8. Cattarin, S.; Musiani, M. J Chim Phis 1996, 93, 650.
9. Hoggins, J. T.; Denivey, M. L. J Electrochem Soc 1984, 131, 2610–2613.
10. Avrami, M. J. J Chem Phys 1938, 7, 1103.